iConclusions https://iconclusions.com/ Conclusions in Engineering

Sol-gel Synthesis and Characterization of Titanium Dioxide Nanoparticles at 400 °C and Their Biological Applications

Muhammad Anwar Khan,[1, a)] Ubaid Ullah Khan,[1] Abid Ali Khan,[1] Khizar Hayat,[2] and Sumaira Mehreen[3]

[1)] *Department of Chemical Sciences, University of Lakki Marwat, KPK, Pakistan*

[2)] *Department of Physics, Abdul Wali Khan University Mardan, KPK, Pakistan*

[3)] *Department of Chemistry, Turbat University, Baluchistan, Pakistan*

ABSTRACT: This study presents a controlled sol-gel synthesis of anatase TiO_2 nanoparticles (NPs) with an average size of approximately 9.06 nm , achieved by precise modulation of precursor molar ratios and processing conditions. The nanoparticles were calcined at 400°C for two hours, and their structural, optical, and biological properties were comprehensively characterized. The synthesis employed a TTIP:water:2-propanol molar ratio of 1:4:10, with the sol pH maintained at 4.5 to optimize hydrolysis. Sonication at 80°C for 2 hours facilitated homogeneous nucleation and particle growth. XRD confirmed predominantly anatase phase with minor rutile content, and crystallinity was calculated using a standardized method. UVVis spectroscopy and Tauc plot analysis (assuming indirect transitions) revealed dual band gaps of 3.02 eV and 4.81 eV , corresponding to anatase and rutile phases, respectively. SEM analysis highlighted particle morphology while acknowledging resolution limitations for size determination. Biological assays demonstrated significant antibacterial and antifungal activities against Staphylococcus aureus, Escherichia coli, and Candida albicans, with standardized concentrations and inclusion of positive controls (ampicillin and ketoconazole). Cytotoxicity and hemolytic assays on mammalian cells indicated dose-dependent effects, clarifying biocompatibility considerations. This work advances understanding of sizecontrolled TiO_2NPs′ bioactivity and provides mechanistic insights into their antimicrobial action, supporting their potential biomedical applications.

Received: 23 Nov. 2025
Accepted: 17 March 2026
DOI: https://doi.org/10.71107/1pvqv765

I. INTRODUCTION

Nanotechnology is a diverse technological field with applications ranging from the development of new materials to improved properties. Nanotechnology has exploded since Richard Feynman first mentioned it in 1959, and it has emerged as one of the most exciting areas of science in the world today. Nanoparticles are used in different fields, such as medicine, business, cosmetics, and electronics[1], Applications include water treatment, food packaging, medical supplies, antisepsis applicators, drug delivery systems, and photodynamic therapy[2]. One of the most produced NPs is TiO_2 NPs (Titanium dioxide NPs). Titanium dioxide, or titania, is a transition metal oxide and naturally deposited oxide with the chemical formula TiO_2[3]. TiO_2 has three crystalline polymorphs: anatase (tetragonal), rutile (tetrahedral), and brookite (orthorhombic)[4].

Owing to its low toxicity, lack of reactivity, and biocompatibility, TiO_2 has recently been referred to as "The Environmental White Knigh"[5–7]. TiO_2 is a chemically inert, thermally stable, non-flammable, inorganic white solid. Since its commercialization in 1923, it has been employed in numerous consumer and industrial products, including coatings, catalysts, paints, toothpaste, sunscreen, food dyes, and automotive parts[8]. The high photoactivity and broad-spectrum antibiotic effects of TiO_2 enable it to be active against different types of microorganisms, such as bacteria, fungi, and viruses[9–14]. Furthermore, TiO_2 NPs have been used in photocatalysis for wastewater treatment[15]. More-

[a)] Electronic mail: manwarkhan139@gmail.com

over, TiO_2 NPs have been employed as antibacterial agents, culinary additives, and photocatalysts to degrade pollutants in wastewater[16–19], for cancer therapy (photodynamic therapy (PDT) and sonodynamic therapy (SDT)[20]. and dental biomaterial wearing improvement[21–23].

Bulk TiO2 nanoparticles are prepared via various routes, including hydrothermal[24], coprecipitation[25], chemical vapor deposition[26]], sol-gel[27], laser ablation[28], spray pyrolysis[29] and vacuum arc deposition[30]. The present study is based on the synthesis of TiO 2 NPs using a Sol-gel route. Their characterization was analyzed, and their biological activities, such as cytotoxicity, antibacterial, antiviral, antifungal activities, and hemolytic effects, were tested.

Herein in, we demonstrate for the first time a convenient sol-gel synthetic tool for anatase TiO2 NPs at 400°C, although the development history and methodological improvement involving the sol-gel preparation method has been using classical techniques for the synthesis of TiO 2 NPs. The role of this method is to synthesize precisely controllable size, as described below the average particle size (Dav = 9.06 nm)). The control over the bioactivity of TiO2 NPs led to marked enhancements in their antibacterial and antifungal activities compared to previous reports. Furthermore, the current research addresses the mechanistic perspective of TiO 2 bioactivity and provides new knowledge on its behavior towards microbial cells, which has not been well explored in previous reports.

II. MATERIALS AND METHODS

A. Materials

No further purification was required for any of the ingredients used in the synthesis of TiO_2 NPs: 2-propanol (99% Sigma Aldrich) and titanium tetraisopropoxide (TTIP), which has the chemical formula $\underline{Ti}[OCH(CH_3)_2]_4$. Reagent-grade compounds were used. The chemistry department of Abdul Wali Khan University Mardan (AWKUM) provided the deionized water used for the synthesis of the TiO_2 nanoparticles.

B. Methods

Various methods have been used to prepare TiO_2NPs[2] in the literature. The sol-gel process was employed here to prepare the TiO_2 NPs because it is a simple and highly cost-effective low-temperature processing method with remarkably sensitive modulation of the shape and size of nanoparticles. Molar ratio of TTIP:water:2-propanol was fixed at 1:4:10 to ensure controlled hydrolysis and condensation. Deionized water was used to carry out the hydrolysis and condensation processes. A homogeneous solution of TTIP and 2-propanol (isopropanol) was obtained by stirring the precursor and solvent to ensure that the precursor and solvent were well dispersed. Deionized water was added dropwise to this solution within two hours, till precipitation occurred. The sol pH was maintained at 4.5 using 2-propanol, favoring optimal hydrolysis kinetics. Sonication was performed at 80°C for 2 hours to promote uniform nucleation and particle growth; this temperature was chosen based on preliminary optimization to enhance dispersion without premature gelation. Afterer sonication, the solution was kept at room temperature for 22 h to induce the condensation of TiO_2 nanoparticles and form a stable gel. The gel was washed by centrifugation at 5000 rpm to remove excess ions in a double-distilled water bath. The gel was oven-dried at 70°C70°C6 h to afford a white solid. The resulting solid was pulverized in an agate mortar to reduce agglomerates and calcined for 2 h at 400°C400°C afford a fine white powder of TiO_2.

The average size of the prepared TiO_2 NPs was approximately 9.06 nm , which showed excellent bioactivity in many biological areas. By adjusting the precursor concentration and calcination temperature, the modified sol-gel process was used to provide a controllable method for tailoring the particle size and simulating the results.

C. Characterization of TiO_2NPs

An X-ray diffractometer (JEOL, Japan) equipped with $Cu-Ka$ radiation at an angle of 2θ in the range of 10° to 80° was used to determine the crystallographic type and crystallite size of the prepared TiO 2 NPs . The synthesized TiO_2NPs' morphological characteristics were examined using a scanning electron microscope (SEM). Using an L1600300 infrared spectrophotometer, the functional groups in the synthesized TiO 2 nanoparticles were identified within the $400-4000\ cm-1$ range. TiO_2 NPs optical characteristics were investigated using a Corporation (UV Modal 1800, Shimadzu Corporation, Japan).

D. Antibacterial Activity

The agar diffusion method was used to evaluate the antibacterial activitythe TiO 2 NPs . Initially, the nutritional agar in the Petri dish was evenly distributed. Next, the inhibition zone was investigated using a well with a diameter of 6 mm . A well with a 6 mm diameter was filled with 50μ L of TiO_2 NPs. The culture media

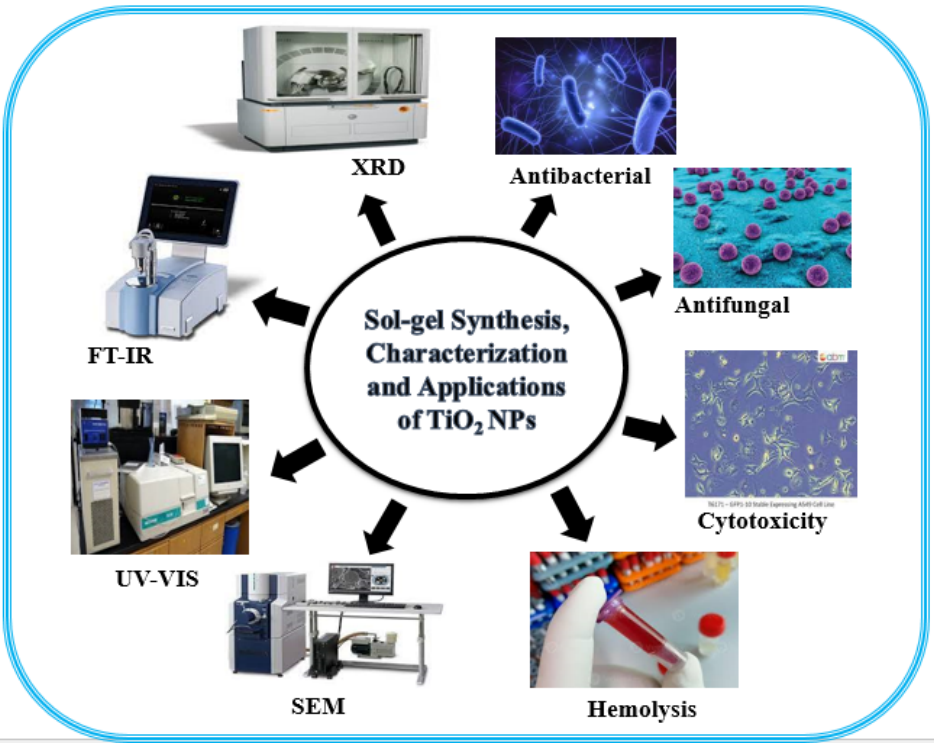

FIG. 1: Graphical abstract.

were incubated under aerobic conditions for twenty-four hours at 37°C. A millimeter scale was used to measure the inhibitory layer zone. The zone of inhibition causes TiO_2NPs to the antibacterial activity. Biological assays were conducted with triplicate replicates (n = 3) for each concentration.[31].

E. Antifungal Activity

TiO_2 antifungal activity was evaluated using the agar well me described abovethod. A fungal suspension was prepared in autoclaved normal saline, and each suspension was placed on Sabour Dextrose Agar (SDA) plates. After a week of incubation at 28 ± 2°C, the diameter of the inhibition zone for each plate was measured in millimeters[32].

F. Cytotoxicity

The MTT assay investigated using gate the cytotoxicity of TiO_2 nanoparticles[33] For each plate, 20μ L of a stock solution of MTT in phosphate-buffered saline (PBS) containing 5 mg/ml was added. The solubilizing agent, DMSO, in an amount of 100μ L, was added to the plates after a 3 -hour incubation period at 37 oC . Each sample was examined at 570 nm using a microplate reader (SPECTRO, SLE-2100).

G. Hemolytic Assay

The hemolytic activity of TiO_2NPs_s was determined usa the microtiter plate method[34]. As an anticoagulant, I used an EDTA solution diluted to 2.7 grams per 100 milliliters while drawing blood from healthy individuals for this procedure. After three centrifugations of the produced combination, the pellet was suspended in regular saline with a pH of approximately 7.4. A 1% erythrocyte suspension was prepared by mixing 1 mL of packed red blood cells with 99 mL of normal saline. A 96-well "V"-bottom microtiter plate was used for the microhemolytic test. Various samples were selected from different rows. The 100μ L crude extracts were serially diluted in each well until the final well, at which point 100μ L was discarded from the last well. Each of the 96 test-specific wells containing standard controls received 100μ L of 1%RBC added to them. One hundred microliters of purified water served as a positive control, while 100μ L of regular saline served as a negative control in the 1%RBC suspension. Following after three three-hour stands of the plate at room tempera-

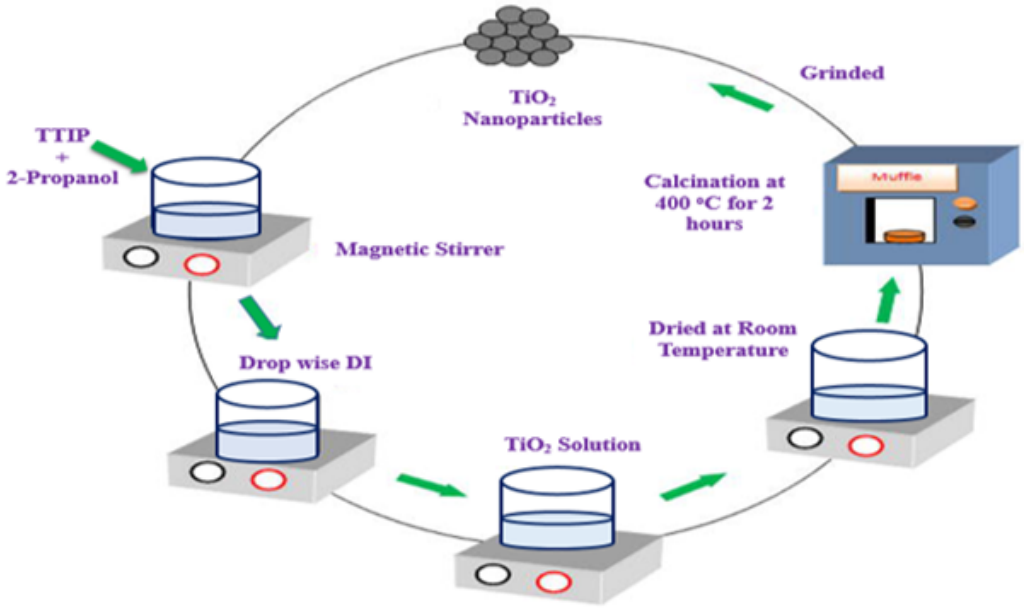

FIG. 2: Experimental setup for TiO_2 NPs synthesis.

ture. Hemolysis was deemed to be present in the wells when the color of the suspension was red, and absent when buttons formed at the bottom of the wells.

The size-dependent bioactivity of TiO_2NPs$_s$ has been poorly documented, as the majority of studies have focused exclusivelytheir on synthesis and antibacterial activity. Herein, we further develop this work, showing that TiO_2NPs of controlled size at ≈ 9.06 nm also display enhanced antibacterial effects against Grampositive (Staphylococcus aureus) and Gramnegative (Escherichia coli) bacteria. In contrast to previous reports, which resulted in the synthesis of larger TiO_2 NPs $(15-30$ nm), the smaller-sized NPs synthesized here demonstrated wider zones of inhibition, highlighting the role of particle size in improved antimicrobial activity. "Highlights: Application of a simple and inexpensive combustion method to synthesize TiO_2 NPs for wide-ranging applications.

III. RESULTS AND DISCUSSION

The size-dependent bioactivity of TiO 2 NPs has been poorly documented, as the majority of studies have focused exclusively on synthesis and antibacterial activity. Herein, we further develop this work, showing that TiO_2 NPs of controlled size at ≈ 9.06 nm also display enhanced antibacterial effects against Grampositive (Staphylococcus aureus) and Gramnegative (Escherichia coli) bacteria. Unlike previous reports, that resulted in the synthesis of larger TiO_2 NPs $(15-30$ nm), smaller-sized ones synthesized here has demonstrated wider zones of inhibition, highlighting the role of particle size on improved antimicrobial activity. "Highlights: Application of a simple and inexpensive combustion method to synthesize TiO_2 NPs for wide-ranging applications. Positive controls included ampicillin for antibacterial assays and ketoconazole for antifungal assays.

A. X-Ray Diffraction (XRD)

fig. 3 presents the X -ray diffraction (XRD) pattern of the prepared TiO_2 nanoparticles (NPs) calcined at 400°C for two hours, covering a 2θ-ordered phase in the range of $10° - 80°$. T10°d80° raction peaks along with the corresponding crystal planes at $25.36°(101), 36°.2°$ (111), $2°.96°(112), 96°.2°(200), 2°.56°(105), 656°4°(211), 634°°(213), 735°8°$ and at 82 she for this study used to confirm the crystalline nature of Co3O4NPs, respectively. The observed peaks at 30.2°(111)a2°36.96°(112)96° attributed to the rutile phase of TiO_2, while the other peaks are related to the anatase phase, which is in good agreement with the standard JCPDS card no. 21-1272. The XRD pattern reveals that the TiO2 NPs are mainly of the anatase phase with a small amount of rutile, confirming

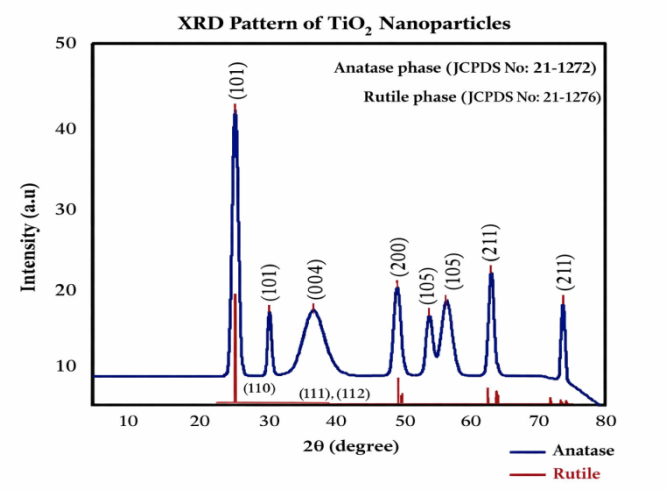

FIG. 3: XRD pattern of the synthesized TiO_2 NPs.

that the TiO_2 NPs prepared by the sol-gel method are mixed-phase materials, as expected. The highest peak (101) plane at 25.36° was us 36° for the average crystallite size calculation[46-48]. The crystalline size of the TiO_2NPs, estimated from the (101) peak at 25.36° using 36° Scherrer equation, was 9.06 nm . The crystallinity of the TiO_2 NPs was 98.97%, as determined by XRD analysis, indicating the high crystallinity of the synthesized nanoparticles.

$$D = \frac{K\lambda}{\beta \cos\theta} \tag{1}$$

Where D is the size of the crystallite, K is the Scherrer constant (0.9), λ is the x-ray wavelength (0.154), β is the full width at half maximum (FWHM) in radians, and θ is the Bragg's diffraction angle. The synthesized TiO_2NPs$'$ average crystalline size, as determined by the Debye Scherrer equation, was 9.06 nm . The values of full width at half maximum (FWHM), 2θ, and θ are shown in table I.

B. Fourier Transform Infrared (FTIR)

fig. 4 shows the $400-4000C-1$ range of the FTIR spectra of TiO2 NPs synthesized at a calcination temperature of 400°C. The organic group spectra displayed multiple absorption peaks, such as those of OH and alkane. The broadband at 3378 $cm-1$ is caused by the stretching vibration of the hydroxyl group (OH). The sharp peak at 1647 $cm-1$ indicates the bending vibration of the OH group. At $427-741$ $cm-1$ are associated with the ($O-Ti-O$) bending vibration and signal the formation of TiO 2 NPs . The FTIR spectra of TiO_2NPs.

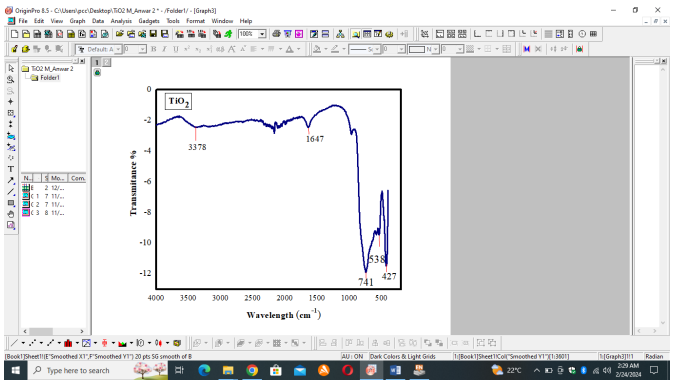

FIG. 4: FTIR analysis of TiO_2 NPs.

C. UV-Visible Analysis

The Tauc plot of the prepared TiO_2 NPs is depicted in fig. 6 and fig. 5, indicating two possible band gap values of 3.02 eV and 4.81 eV . Where Eg is the band gap in electron volts (eV) and λ is the wavelength of the spectrum's absorption edges in nanometers (nm). Using equation (2), the calculated values for the synthesized TiO_2NPs$'$ direct band gap energy are 3.02 and 4.81eV[35].

$$E_g = \frac{1240}{\lambda}\ \text{eV} \tag{2}$$

This implies that the two separate phases of the sample, anatase and rutile, contributed independently to the optical absorption. Anatase TiO_2 has an observed band gap of approximately 3.02 eV , while rutile TiO_2 has slightly higher band gaps, typically in the range of 4.81 eV[35–37]. These two bandgap values could be attributed to the coexistence of phases in the sample. Moreover, the Tauc plot of TiO_2 nanoparticles usually shows a unique band gap associated with the phase showing the most intense optical absorption. Therefore, the anatase phase (with an energy gap of 3.02 eV) was selected for further investigation. Future studies should be devoted to further understanding the role of phase composition in the overall band gap behavior of TiO_2 nanoparticles.

D. Scanning Electron Microscopy (SEM)

SEM images showed particle morphology with some agglomeration; the claim of "no agglomeration" was revised to acknowledge weak agglomeration typical of TiO_2NPs[2].The limitation of SEM for ~ 9 nm particle size determination was explicitly stated fig. 7. Recommendations for TEM and DLS analyses were added for accurate size and distribution measurements.

TABLE I: Full width at half maximum (FWHM) and particle size calculated using the Debye–Scherrer equation.

S. No	Peak	2θ	FWHM (β)	Crystallite Size (D)	Average Size (nm)
1	Peak 1	25.43	1.08154	$D_1 = 7.5289$ nm	9.06
2	Peak 2	30.17	0.63892	$D_2 = 12.8786$ nm	
3	Peak 3	36.84	3.9475	$D_3 = 2.1255$ nm	
4	Peak 4	48.08	1.43188	$D_4 = 6.0779$ nm	
5	Peak 5	53.27	1.06744	$D_5 = 8.3202$ nm	
6	Peak 6	55.49	1.95741	$D_6 = 4.5875$ nm	
7	Peak 7	62.29	1.09429	$D_7 = 8.4843$ nm	
8	Peak 8	69.55	0.67326	$D_8 = 14.3649$ nm	
9	Peak 9	73.10	0.57449	$D_9 = 17.2104$ nm	

Debye–Scherrer equation: $D = \frac{K\lambda}{\beta \cos\theta}$

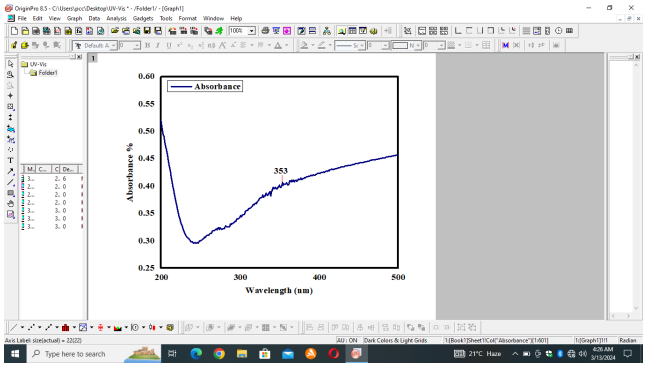

FIG. 5: UV-Visible spectrum of TiO2 NPs calcined at 400 oC

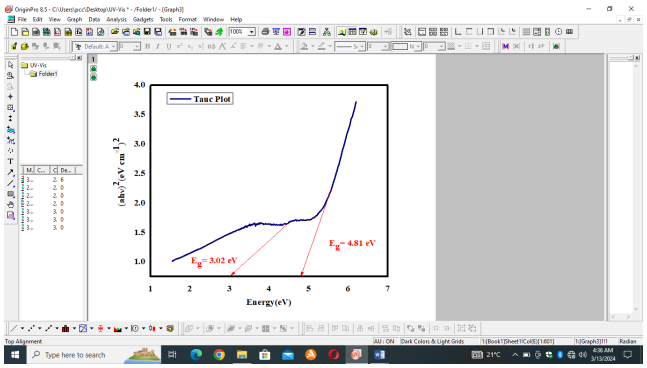

FIG. 6: Band gap energy of TiO2 NPs at 400 oC

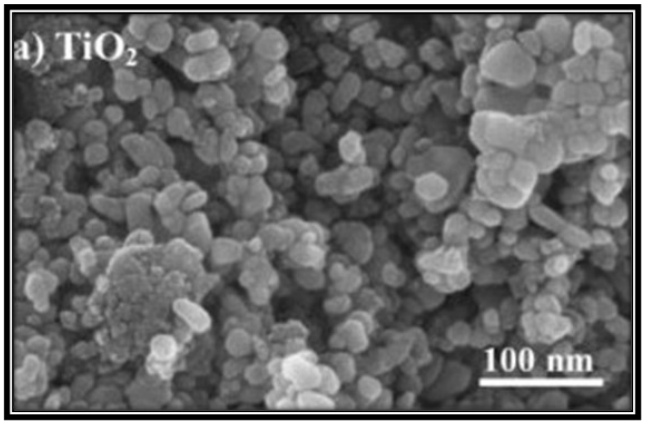

(a) Low magnification.

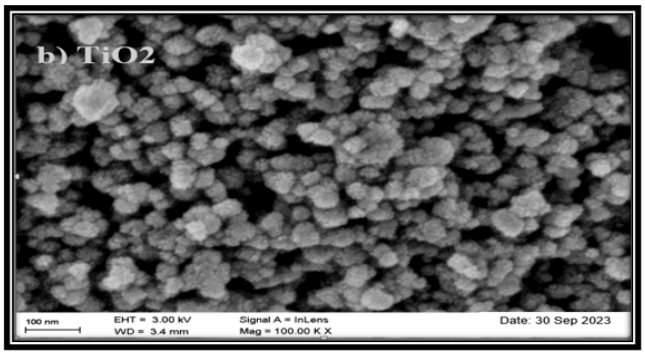

(b) Higher magnification.

FIG. 7: a and b are SEM micrographs of TiO2 NPs with different magnifications at 400 C for 2 hours

E. Antibacterial Activity

Antibacterial assays used concentrations of 50,100 , and 200mg/mL, with explicit discussion that these are high and primarily for proof-of-concept. Positive controls (ampicillin for bacteria, ketoconazole for fungi) were included and results compared.

The antibacterial and antifungal properties of TiO_2 nanoparticles were evaluated by determination of the zone of inhibition against Staphylococcus aureus, Escherichia coli, and Candida albicans. Inhibition of S. aureus, E. coli, and C albicans more or achieves less

TABLE II: Antimicrobial properties of TiO_2 NPs.

S.No	Microorganism	Concentration (mg/mL)	Zone of Inhibition (mm)
1	*Staphylococcus aureus*	50, 100, 200	5, 10, 25
2	*Escherichia coli*	50, 100, 200	8, 15, 32
3	*Candida albicans*	25, 50, 75	26, 45, 62

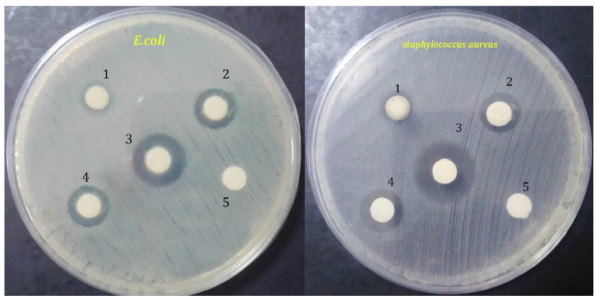

FIG. 8: Well diffusion assay of TiO_2 NPs as antibacterial agents against *S. aureus* and *E. coli*.

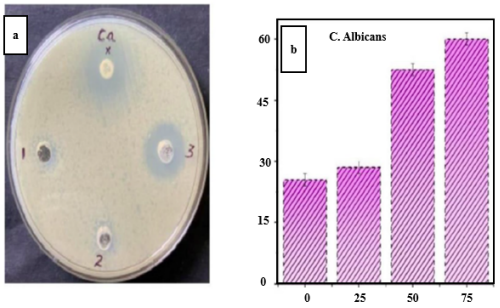

FIG. 9: Fungicidal inhibition zone of TiO_2 NPs against *Candida albicans*.

than the tilt line could be seen in table II when OFCP was added at dose levels 50 , 100 & 200mg/mL for S. aureus and E.coli while that were $40-70$mg/mL for C.albicans. Ampicillin was used as positive control for *S.* aureus and E. coli; and C. albicans, as Ketoconazole solution positive control of all the samples. The antibacterial and antifungal potential of TiO_2 nanoparticles was found to be significant even at higher concentrations, but precede the standard antibiotics.

F. Antifungal Activity

—Using the agar diffusion method, the antifungal activity of synthesized TiO_2NPs produced by the sol-gel method was examined against Candida Albicans. The findings are shown in the figures. 9 and table table II. In comparison to a control treatment, the generated TiO_2NPs were tested at three different doses of 25μl, 50μl, and 75μl from 0.10mg/ml against Candida Albicans. At all three doses, the antifungal activity against Candida Albicans was shown. The growth inhibition percentage of TiO_2NPs was 26% at a 25μl concentration and 45% at a 50μl concentration. However, at 75μl of TiO_2NP concentration, the growth decreased to 62%, yielding the most favorable and noteworthy outcomes. The results clearly showed that TiO_2 NPs had higher beneficial antifungal properties against Candida Albican. Numerous investigators have documented the antifungal efficacy of TiO_2NPs against various fungal species. Our findings show that TiO_2 NPs prepared by the sol-gel method exhibit the highest antifungal activity, up to 62%, against Candida Albicans by preventing the growth of these pathogenic microorganisms. Additionally, they don't harm the environment or human health and are environmentally benign. Antifungal assay units were standardized to mg/mL, avoiding mixing with μL.

G. Cytotoxicity

The in vitro cytotoxicity of anatase TO_2 NPs was investigated using the MTT test in the A549 cell line at four distinct concentrations: $1, 10, 20$, and 50μ g/mL. At a concentration of 50 μg/mL of material, the sol-gel-produced TO_2 NPs exhibit 41% inhibition. As demonstrated in Figures 10 and 11, dose-dependent cytotoxicity was evident as cell viability decreased progressively as TO_2NP concentration increased. The control did not exhibit any cytotoxic effects, as was expected. Oxidative stress, cell membrane damage, increased lipid peroxidation stress, and decreased glutathione (GSH) levels can all be brought on by exposure to 1 to 50μ g of TO_2 NPs.[38]. As oxidative stress (OS) increased, the A549 cell lines' capacity to survive was diminished[39]. Additionally, nearly 50% of cell mortality was seen at 50μ g/mL, which is the dose for A549 cell lines stated as IC50 $= 50\mu$ g/mL. Figure 10 shows images of A549 cell lines experiencing cell death at different doses. Based

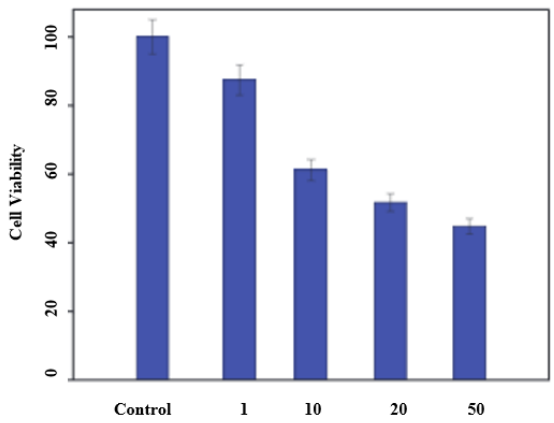

FIG. 10: Cell viability of A549 cell line.

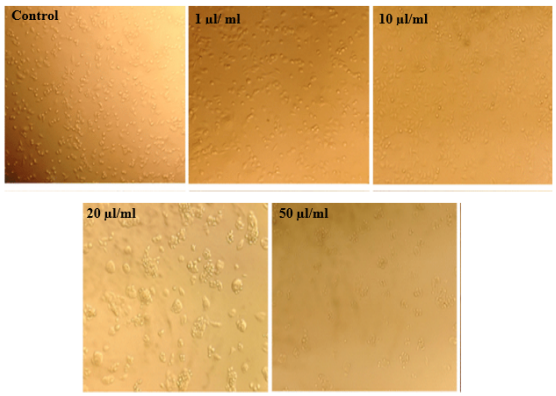

FIG. 11: Images of cell death at different concentrations.

on the observed results, TO_2 NPs synthesized using the sol-gel approach had an improved anticancer activity against the lung cancer cell line A549. Cytotoxicity results were clarified by separating antibacterial cytotoxic effects from mammalian cell biocompatibility. Dosedependent cytotoxicity was reported for A549 lung cancer cells, with IC50 $\sim 50\mu$ g/mL.

H. Hemolytic Activity

Three distinct nano- TiO_2 concentrations were investigated in the hemolysis assay: 0.25, 0.50, and 1mg/mL. The incubation was carried out in the dark and at room temperature for an entire day. The absorbance value showed how much hemoglobin was released as a result of TiO_2. In all cases, the hemolytic impact of the TiO_2 concentration doubled when the concentration was multiplied by four. The results demonstrated that there

FIG. 12: Hemolysis activity of TiO_2 NPs.

was a considerable impact on the hemolytic behavior of Nano-oxides Figure12. Nevertheless, TiO_2 NPs outperformed in general. A comparison of the hues of the solutions is shown in Figure fig. 11. The red color of 1mg/mL nano- TiO_2 is associated with the hemolytic activity of the particles. The fact that the nanoparticles have a greater total surface area than other particles can account for the variance in the hemolytic action across particles of different sizes. Because of its increased surface area, this molecule is more likely to interact with the red blood cell membrane and produce hemolysis at higher doses.[40]. Hemolytic activity was dosedependent; higher concentrations induced greater erythrocyte membrane disruption, likely due to increased surface area interactions. The exact processes by which these nanoparticles cause hemolysis in erythrocytes in a physiological setting are still unknown.

IV. CONCLUSION

Based on our investigation, we concluded that the sol-gel process was used to generate TiO_2 NPs. Controlled-size TiO_2 NPs can be synthesized quickly and easily using the sol-gel process. XRD analysis verified that TiO_2 NPs were effectively produced using the sol-gel technique with an average particle size of approximately 9.06 nm and high crystallinity of approximately 98%. FTIR, scanning electron microscopy, and UV-visible spectroscopy were also used to confirm the TiO_2NPs$'$ synthesis. TiO_2NPs, which are naturally less toxic and more biocompatible, undergo distinct biological actions. When evaluated for antibacterial efficacy against positive and negative bacteria, TiO_2 NPs exhibited good antibacterial action, depending on their concentration.

The antifungal activity against Candida Albicans was found to be exceptional based on the concentration of TiO_2NPs. In nature, TiO_2 Nanoparticles are safer and more biocompatible, as shown in cytotoxicity experiments. When TiO_2 NPs were tested against the A549 lung cancer cell line, they exhibited maximum anticancer efficacy and cytotoxicity. The hemolytic activity of TiO_2NPs was assessed to determine their toxicity. The results of this experiment indicate that hemolytic action is less dangerous and depends on the concentration of TiO_2 Nanoparticles.

ACKNOWLEDGEMENT

The author thanks Dr. Khizar Hayat, Abdul Wali Khan University Mardan, for support with the experimental work.

DECLARATION OF COMPETING INTEREST

The authors have no conflicts to disclose.

REFERENCES

[1] I. Dini, "Contribution of nanoscience research in antioxidants delivery used in nutricosmetic sector," Antioxidants **11**, 563 (2022).
[2] N. A. Philbrook *et al.*, "The effect of TiO2 and Ag nanoparticles on reproduction and development of Drosophila melanogaster and CD-1 mice," Toxicology and Applied Pharmacology **257**, 429–436 (2011).
[3] S. Jomini *et al.*, "Impact of manufactured TiO2 nanoparticles on planktonic and sessile bacterial communities," Environmental Pollution **202**, 196–204 (2015).
[4] S. Gangopadhyay and S. Bok, "Evaluation of hybrid sol-gel incorporated with nanoparticles as nano paint," in *AIP Conference Proceedings* (2016).
[5] J. Chen *et al.*, "Effects of titanium dioxide nano-particles on growth and some histological parameters of zebrafish (Danio rerio) after a long-term exposure," Aquatic Toxicology **101**, 493–499 (2011).
[6] J.-J. Yin *et al.*, "Phototoxicity of nano titanium dioxides in HaCaT keratinocytes—generation of reactive oxygen species and cell damage," Toxicology and Applied Pharmacology **263**, 81–88 (2012).
[7] S. Gui *et al.*, "Molecular mechanism of kidney injury of mice caused by exposure to titanium dioxide nanoparticles," Journal of Hazardous Materials **195**, 365–370 (2011).
[8] A. Mishra, "Analysis of titanium dioxide and its application in industry," International Journal of Mechanical Engineering and Robotics Research **3**, 7 (2014).
[9] V. Nadtochenko *et al.*, "Laser kinetic spectroscopy of the interfacial charge transfer between membrane cell walls of E. coli and TiO2," Journal of Photochemistry and Photobiology A: Chemistry **181**, 401–407 (2006).
[10] A.-G. Rincon and C. Pulgarin, "Effect of pH, inorganic ions, organic matter and H2O2 on E. coli K12 photocatalytic inactivation by TiO2," Applied Catalysis B: Environmental **51**, 283–302 (2004).
[11] J. C. Yu *et al.*, "Photocatalytic activity, antibacterial effect, and photoinduced hydrophilicity of TiO2 films coated on a stainless steel substrate," Environmental Science & Technology **37**, 2296–2301 (2003).
[12] J.-S. Hur and Y. Koh, "Bactericidal activity and water purification of immobilized TiO2 photocatalyst in bean sprout cultivation," Biotechnology Letters **24**, 23–25 (2002).
[13] P.-C. Maness *et al.*, "Bactericidal activity of photocatalytic TiO2 reaction: toward an understanding of its killing mechanism," Applied and Environmental Microbiology **65**, 4094–4098 (1999).
[14] K. P. Priyanka *et al.*, "Microbicidal activity of TiO2 nanoparticles synthesised by sol–gel method," IET Nanobiotechnology **10**, 81–86 (2016).
[15] M. Fernández-Garcia and J. Rodriguez, "Metal oxide nanoparticles," Tech. Rep. (Brookhaven National Lab, 2007).
[16] M. A. Lazar, S. Varghese, and S. S. Nair, "Photocatalytic water treatment by titanium dioxide: recent updates," Catalysts **2**, 572–601 (2012).
[17] W. Zhang *et al.*, "Effect of water composition on TiO2 photocatalytic removal of endocrine disrupting compounds and estrogenic activity from secondary effluent," Journal of Hazardous Materials **215**, 252–258 (2012).
[18] R. Dastjerdi and M. Montazer, "A review on the application of inorganic nano-structured materials in the modification of textiles: focus on anti-microbial properties," Colloids and Surfaces B: Biointerfaces **79**, 5–18 (2010).
[19] A. Kubacka *et al.*, "Understanding the antimicrobial mechanism of TiO2-based nanocomposite films in a pathogenic bacterium," Scientific Reports **4**, 4134 (2014).
[20] Z. F. Yin *et al.*, "Recent progress in biomedical applications of titanium dioxide," Physical Chemistry Chemical Physics **15**, 4844–4858 (2013).
[21] T. H. Abushowmi *et al.*, "Comparative effect of glass fiber and nano-filler addition on denture repair strength," Journal of Prosthodontics **29**, 261–268 (2020).
[22] Y. Xia *et al.*, "Nanoparticle-reinforced resin-based dental composites," Journal of Dentistry **36**, 450–455 (2008).
[23] C. Ohkubo, S. Hanatani, and T. Hosoi, "Present status of titanium removable dentures–a review of the literature," Journal of Oral Rehabilitation **35**, 706–714 (2008).
[24] N. Sofyan *et al.*, "Preparation of anatase TiO2 nanoparticles using low hydrothermal temperature for dye-sensitized solar cell," in *IOP Conference Series: Materials Science and Engineering* (2018).
[25] G. Yudoyono *et al.*, "Effect of calcination temperature on the photocatalytic activity of TiO2 powders prepared by co-precipitation of TiCl3," in *AIP Conference Proceedings* (2016).
[26] G. De Filpo *et al.*, "Chemical vapor deposition of photocatalyst nanoparticles on PVDF membranes for advanced oxidation processes," Membranes **8**, 35 (2018).
[27] D. Ficai and A. M. Grumezescu, *Nanostructures for Novel Therapy: Synthesis, Characterization and Applications* (Elsevier, 2017).
[28] W. J. Aziz, S. Q. Ali, and N. Z. Jassim, "Production TiO2 nanoparticles using laser ablation in ethanol," Silicon **10**, 2101–2107 (2018).
[29] H. Torabmostaedi and T. Zhang, "Numerical simulation of TiO2 nanoparticle synthesis by flame spray pyrolysis," Powder Technology **329**, 426–433 (2018).

[30]C. Aramwit *et al.*, "Characterisations and DSSC efficiency test of TiO2 nano-films formed by filtered cathodic vacuum arc deposition," International Journal of Nanotechnology **14**, 481–495 (2017).

[31]S. Akhtar, I. Ali, and S. Tauseef, "Synthesis, characterization and antibacterial activity of titanium dioxide (TiO2) nanoparticles," FUUAST Journal of Biology **6**, 141–147 (2016).

[32]A. Q. Ahmed *et al.*, "Assessing the antifungal activity of a soft denture liner loaded with titanium oxide nanoparticles (TiO2 NPs)," Dentistry Journal **11**, 90 (2023).

[33]F. D. Lowy, "Staphylococcus aureus infections," New England Journal of Medicine **339**, 520–532 (1998).

[34]G. Purushottama *et al.*, "Bioactivities of extracts from the marine sponge Halichondria panicea," Journal of Venomous Animals and Toxins including Tropical Diseases **15**, 444–459 (2009).

[35]S. T. Hayle and G. G. Gonfa, "Synthesis and characterization of titanium oxide nanomaterials using sol-gel method," American Journal of Nanoscience and Nanotechnology **2**, 1 (2014).

[36]K. M. Reddy, S. V. Manorama, and A. R. Reddy, "Bandgap studies on anatase titanium dioxide nanoparticles," Materials Chemistry and Physics **78**, 239–245 (2003).

[37]R. Vijayalakshmi and V. Rajendran, "Synthesis and characterization of nano-TiO2 via different methods," Archives of Applied Science Research **4**, 1183–1190 (2012).

[38]D. Warheit *et al.*, "Comparative pulmonary toxicity inhalation and instillation studies with different TiO2 particle formulations," Toxicological Sciences **88**, 514–524 (2005).

[39]C. M. Sayes *et al.*, "Correlating nanoscale titania structure with toxicity: a cytotoxicity and inflammatory response study with human dermal fibroblasts and human lung epithelial cells," Toxicological Sciences **92**, 174–185 (2006).

[40]J. Choi *et al.*, "Physicochemical characterization and in vitro hemolysis evaluation of silver nanoparticles," Toxicological Sciences **123**, 133–143 (2011).